Polarized spectroscopy of electric and magnetic dipole transitions of Europium (III) ions in C_2 sites

Polarized spectroscopy of electric and magnetic dipole transitions of Europium (III) ions in C_2 sites

A Volokitina[1,2], P Loiko[3], E Dunina[4], A Kornienko[4], J M Serres[2], M Aguiló[2], F Díaz[2], A Pavlyuk[5] and X Mateos[2,6]

[1] ITMO University, 49 Kronverkskiy Pr., 197101 St. Petersburg, Russia
[2] Universitat Rovira i Virgili, Física i Cristal·lografia de Materials i Nanomaterials (FiCMA-FiCNA), Marcel.li Domingo 1, 43007 Tarragona, Spain
[3] Centre de Recherche sur les Ions, les Matériaux et la Photonique (CIMAP), UMR 6252 CEA-CNRS-ENSICAEN, Université de Caen Normandie, 6 Boulevard Maréchal Juin, 14050 Caen Cedex 4, France
[4] Vitebsk State Technological University, 72 Moskovskiy Pr., 210035 Vitebsk, Belarus
[5] A.V. Nikolaev Institute of Inorganic Chemistry, Siberian Branch of Russian Academy of Sciences, 3 Lavrentyev Ave., 630090 Novosibirsk, Russia
[6] Serra Húnter Fellow

anna.itmo@gmail.com

Abstract. Polarization anisotropy of luminescent properties of europium (III) ions in low-symmetry C_2 sites is studied using monoclinic (sp. gr. *C*2/*c*) tungstate crystal $KY(WO_4)_2$. The $^5D_0 \rightarrow {}^7F_J$ (where $J = 0...6$) transitions are characterized for the principal light polarizations. Polarization selection rules for the magnetic dipole $^5D_0 \rightarrow {}^7F_1$ transition are presented. The stimulated-emission cross-sections for Eu^{3+} ions relevant for laser operation are determined.

1. Introduction

Trivalent europium ions, Eu^{3+} or Eu (III), possessing an electronic configuration of $[Xe]4f^6$ are well-known for their emissions in the visible owing to transitions from a metastable (long-living) $^5D_0$ state to a group of lower-lying ^7F_J ($J = 0...6$) multiplets ($^7F_0$ is the ground-state). Among them, the electric dipole (ED) transition to the $^7F_2$ state falling in the red spectral range (~610 nm) typically dominates in the emission spectrum. This determines the applications of Eu^{3+}-doped materials as red phosphors with high colour purity [1,2], e.g., commercialized Eu^{3+}:Y_2O_3S. Note that europium also exhibits another oxidation state, Eu^{2+}. Eu^{2+}-doped materials are used as blue phosphors [3].

Eu^{3+} ions are also attractive as structural probes [4]. First, the transition $^5D_0 \rightarrow {}^7F_0$ is both electric dipole and magnetic dipole (MD) forbidden. Its observation is due to J–J-mixing in the local field [5]. Both the emitting and the terminal levels are non-degenerate ($J = 0$), so that the number of emission lines corresponds to the number of non-equivalent Eu^{3+} sites in the host lattice. Second, the transition $^5D_0 \rightarrow {}^7F_1$ is of purely MD nature (so that its probability is weakly dependent on the host), while the spectrally adjacent transition $^5D_0 \rightarrow {}^7F_2$ is of purely ED nature (it is a hypersensitive one, i.e., its probability depends on the local site symmetry and its distortion). The ratio $R = I_{ED}(0\rightarrow2)/I_{MD}(0\rightarrow1)$ is known as an asymmetry parameter [4]: if Eu^{3+} site does not exhibit a centre of inversion, $R >> 1$.

Finally, Eu^{3+}-doped crystals are also suitable for direct generation of red laser emission [6-8]. Recently, Loiko *et al.* reported on a highly-efficient Eu laser in a stoichiometric compound, namely a monoclinic $KEu(WO_4)_2$ crystal, operating on the $^5D_0 \rightarrow {}^7F_4$ transition and delivering watt-level output at ~703 nm (in the deep-red spectral range) [9], which stimulated the study of polarized emission properties of Eu^{3+}-doped crystals.

Among the host matrices intended for Eu^{3+} doping, monoclinic double tungstates (MDTs) with a chemical formula $KRE(WO_4)_2$ (where RE = Gd, Y, Lu) appear very suitable. Their advantages are: (i) high available doping concentrations up to stoichiometric compositions, (ii) long RE^{3+} - RE^{3+} interatomic distances leading to weak concentration quenching of luminescence, and (iii) strong polarization anisotropy of emission properties [9,10]. Considering the great potential of Eu^{3+}-doped MDT crystals for the development of red and deep-red lasers operating on different $^5D_0 \rightarrow {}^7F_J$ transitions, it is relevant to study in detail the anisotropy of transitions in emission.

In the present work, we have studied in detail the polarization anisotropy of the ED and MD transitions of Eu^{3+} ions in the monoclinic $KY(WO_4)_2$ crystal.

2. Experimental

The studied crystal, europium-doped potassium yttrium double tungstate, 2 at.% $Eu:KY(WO_4)_2$, was grown from the flux by Dr. Anatoly Pavlyuk. The so-called Low Temperature Gradient (LTG) method was used. Potassium ditungstate ($K_2W_2O_7$) was used as a solvent. An undoped seed was oriented along the [010] axis. The thermal gradients in the flux were below 0.1 °C/cm. More details can be found elsewhere [10]. A photograph of the as-grown crystal is shown in Figure 1.

Figure 1. Photograph of the 2 at.% $Eu:KY(WO_4)_2$ crystal, the growth direction is along the [010] axis.

$Eu:KY(WO_4)_2$ is monoclinic (sp. gr. C^6_{2h} - $C2/c$) and optically biaxial. The crystal was oriented by single-crystal X-ray diffraction. The orientation of the optical indicatrix frame is the following [11]: the N_p axis is parallel to the ***b***-axis and the N_m and N_g ones are lying in the orthogonal ***a-c*** plane, the angle N_g ^ ***c*** is 18.5° (out of the monoclinic angle). The principal optical directions N_p, N_m and N_g are selected according to the relation for the corresponding refractive indices, $n_p < n_m < n_g$.

In the $KY(WO_4)_2$ lattice, the Eu^{3+} ions are replacing for the Y^{3+} cations in a single type of sites with C_2 symmetry and VIII-fold oxygen coordination (the corresponding ionic radii are R_Y^{VIII} = 1.019 Å and R_{Eu}^{VIII} = 1.066 Å [12]). This coordination depicts a square antiprism polyhedron.

Polarized luminescence spectra of Eu^{3+} ions were measured at room temperature (RT, 293 K) using a confocal Raman microscope (InVia, Renishaw) equipped with an Ar^+ ion laser as an excitation source (λ_{exc} = 488.0 nm), a ×50 Leica microscope objective, a 1800 l/mm grating, a CCD detector, an edge filter and a set of a polarizer and an analyser. The spectral resolution was ~1 cm^{-1}.

3. Results and discussion

An unpolarised overview luminescence spectrum of Eu^{3+} ions was measured as shown in Figure 2. The observed emission bands are due to the $^5D_0 \rightarrow {}^7F_J$ transitions, at 581 nm ($J = 0$), 590-596 nm ($J = 1$), 613-627 nm ($J = 2$), 649-658 nm ($J = 3$), 694-707 nm ($J = 4$), 742-764 nm ($J = 5$) and 803-840 nm ($J = 6$). No spectroscopic evidences of Eu^{2+} species were found. The measured luminescence lifetime of the $^5D_0$ state was 430 μs [10]. The $^5D_0 \rightarrow {}^7F_2$ transition dominated in the spectrum and it determined the red colour of the luminescence (CIE 1931 colour coordinates, $x = 0.670$, $y = 0.329$). The dominant emission wavelength λ_d was calculated to be 613 nm and the colour purity p exceeded 98%.

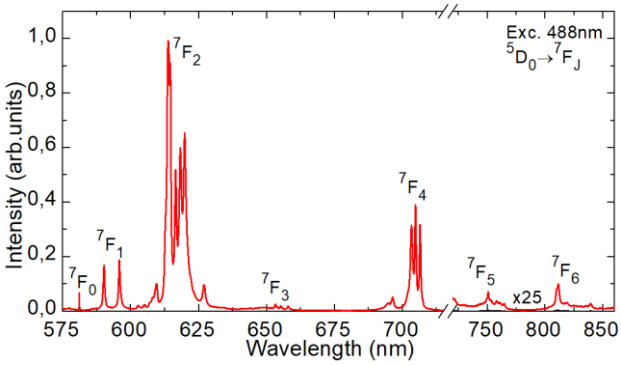

Figure 2. Unpolarized overview luminescence spectrum of Eu^{3+} ions in $KY(WO_4)_2$, $\lambda_{exc} = 488$ nm.

The polarization anisotropy of the emission properties is of particular interest for transitions suitable for laser operation, namely $^5D_0 \rightarrow {}^7F_2$ (red emission) and $^5D_0 \rightarrow {}^7F_4$ (deep-red emission). Both are of pure ED nature. First, polarized luminescence spectra were measured for $\boldsymbol{E} \parallel N_p$, N_m and N_g. Then, stimulated-emission (SE) cross-sections, σ_{SE}, were calculated by the Füchtbauer-Ladenburg (F-L) formula [13]:

$$\sigma^{i}_{SE}(\lambda) = \frac{\lambda^5}{8\pi\langle n\rangle^2 c\tau_{rad}} \frac{W_i(\lambda)B(JJ')}{(1/3)\sum_{j=p,m,g}\int \lambda W_j(\lambda)d\lambda}, \quad (1)$$

where, the $i, j = p, m, g$ indices mark the polarization state, λ is the light wavelength, $\langle n \rangle$ is the mean refractive index, c is the speed of light, $\tau_{rad} = 464$ μs [10] is the radiative lifetime of the emitting state ($^5D_0$), $B(JJ') = 83.7\%$ ($0 \rightarrow 2$) and 12.8% ($0 \rightarrow 4$) [10] are the luminescence branching ratios for the J $\rightarrow$ J' transitions and $W_i(\lambda)$ is the luminescence spectrum for the i-th polarization. The $B(JJ')$ and τ_{rad} values were calculated previously using the Judd-Ofelt theory [10].

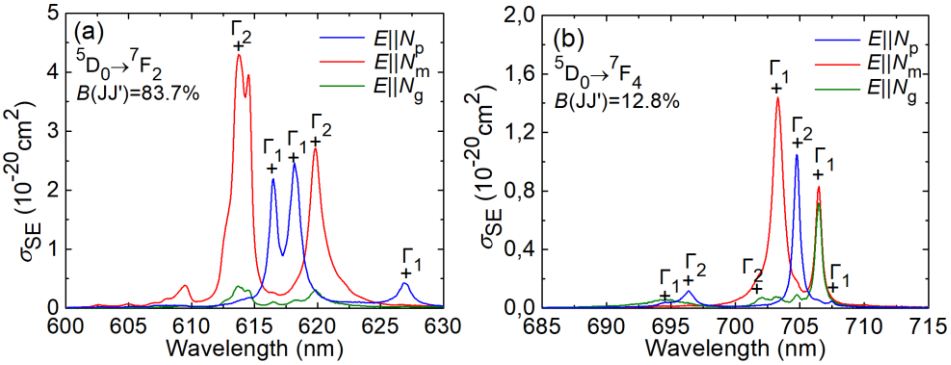

Figure 3. Stimulated-emission (SE) cross-section, σ_{SE}, spectra for electric-dipole (ED) transitions **(a)** $^5D_0 \rightarrow {}^7F_2$ and **(b)** $^5D_0 \rightarrow {}^7F_4$ of Eu^{3+} ions in the monoclinic $KY(WO_4)_2$ crystal for light polarizations $\boldsymbol{E} \parallel N_p$, N_m and N_g. "+" marks electronic transitions, $\Gamma_{1(2)}$ – irreducible representations corresponding to sub-levels of the ^7F_J multiplets.

The σ_{SE} spectra are shown in Figure 3(a,b). They are strongly polarized. For the $^5D_0 \rightarrow {}^7F_2$ transition falling in the red spectral range, the highest SE cross-sections correspond to light polarization $\boldsymbol{E} \parallel N_m$. The two prominent emission peaks are at 613.7 nm (4.31×10^{-20} cm^2) and 619.8 nm (2.72×10^{-20} cm^2). For the former broader and more intense peak, the emission bandwidth (full width at half maximum, FWHM) is 1.6 nm. Another favorable light polarization is $\boldsymbol{E} \parallel N_p$. Again, two intense emission peaks are observed at 616.5 nm (2.20×10^{-20} cm^2) and 618.2 nm (2.46×10^{-20} cm^2). The principal polarization $\boldsymbol{E} \parallel N_g$ corresponds to much lower SE cross-sections and it is less interesting for laser applications.

For the $^5D_0 \rightarrow {}^7F_4$ transition corresponding to deep-red emissions, the highest SE cross-sections also correspond to light polarization $\boldsymbol{E} \parallel N_m$. Two intense emission peaks at 703.3 nm (1.44×10^{-20} cm^2) and 706.5 nm (0.83×10^{-20} cm^2) are observed; the emission bandwidth (FWHM) of the former peak is 1.0 nm. For $\boldsymbol{E} \parallel N_p$, there is only one intense peak at 704.8 nm (1.05×10^{-20} cm^2).

For Eu^{3+} ions in C_2 sites, every $^{2S+1}L_J$ multiplet (with integer J) is split into a total of $2J + 1$ Stark sub-levels with irreducible representations Γ_1 and Γ_2, cf. Table 1.

Table 1. Expected number of Stark sub-levels for Eu^{3+} ions in C_2 sites and the corresponding irreducible representations.

$^{2S+1}L_J$ (Eu^{3+})	Γ ($2J + 1$)	$^{2S+1}L_J$ (Eu^{3+})	Γ ($2J + 1$)
$^7F_0$	Γ_1 (1)	$^7F_4$	$5\Gamma_1+4\Gamma_2$ (9)
$^7F_1$	$2\Gamma_1+\Gamma_2$ (3)	$^7F_5$	$5\Gamma_1+6\Gamma_2$ (11)
$^7F_2$	$3\Gamma_1+2\Gamma_2$ (5)	$^7F_6$	$7\Gamma_1+6\Gamma_2$ (13)
$^7F_3$	$3\Gamma_1+4\Gamma_2$ (7)	$^5D_0$	Γ_1 (1)

Table 2. Polarization dependent selection rules for ED J → J' transitions of Eu^{3+} ions in the monoclinic $KY(WO_4)_2$ crystal, C_2 – 2-fold symmetry axis, *p*, *m*, *g* – polarization states.

J → J'	Γ_1	Γ_2
Γ_1	$\boldsymbol{E} \parallel C_2$ (*p*)	$\boldsymbol{E} \perp C_2$ (*m*, *g*)
Γ_2	$\boldsymbol{E} \perp C_2$ (*m*, *g*)	$\boldsymbol{E} \parallel C_2$ (*p*)

The polarization selection rules for ED J → J' transitions of Eu^{3+} ions are listed in Table 2. For the monoclinic $KY(WO_4)_2$ crystal, the point group is 2/*m*. The 2-fold symmetry axis (C_2) is parallel to the crystallographic ***b***-axis ($C_2 \parallel N_p$). It is orthogonal to the mirror plane coinciding with the ***a-c*** plane and, consequently, containing the N_m and N_g axes. The polarization selection rules are different for light polarized along the 2-fold axis ($\boldsymbol{E} \parallel N_p$) and orthogonal to it ($\boldsymbol{E} \parallel N_m, N_g$). This agrees well with the observed polarization anisotropy of ED transitions of Eu^{3+} ions, cf. Figure 3.

Let us now discuss the $^5D_0 \rightarrow {}^7F_{0,1}$ transitions of Eu^{3+} ions in $KY(WO_4)_2$ which correspond to the "structural probe" role of these species. For the ED and MD forbidden $^5D_0 \rightarrow {}^7F_0$ transition, a single narrow emission line was observed at 581.3 nm (17203 cm^{-1}) for light polarization $\boldsymbol{E} \parallel N_p$, Figure 4(a). This agrees with a single type of sites for Eu^{3+} ions. As both the emitting and the terminal levels for this transition are non-degenerated and the irreducible representation corresponding to the single Stark sub-level is Γ_1 (Table 1), according to the polarization selection rules (cf. Table 2), it can be observed only for light polarized along the 2-fold symmetry axis (i.e., along the N_p-axis).

The polarized luminescence spectra corresponding to the $^5D_0 \rightarrow {}^7F_1$ Eu^{3+} transition are shown in Figure 4(b). In our experiments, it was observed that the relative intensity and position of the emission lines depend not only on the polarization of luminescence ***E***, but also on its propagation direction ***k*** (like for Raman spectra). To clarify this, Porto's notations were used: $\boldsymbol{k}_{exc}(\boldsymbol{E}_{exc}\boldsymbol{E}_{lum})\boldsymbol{k}_{lum}$, where $\boldsymbol{k}_{exc}$ and $\boldsymbol{k}_{lum}$ are the directions of propagation of the excitation light and luminescence, respectively (in our case they correspond to the same direction in the crystal because of the confocal geometry), and $\boldsymbol{E}_{exc}$ and

$\boldsymbol{E}_{\text{lum}}$ are the polarization states of the excitation light and luminescence, respectively. In Figure 4(b), the spectra are grouped according to the polarization state of luminescence ($\boldsymbol{E}_{\text{lum}}$, *p*, *m* or *g*).

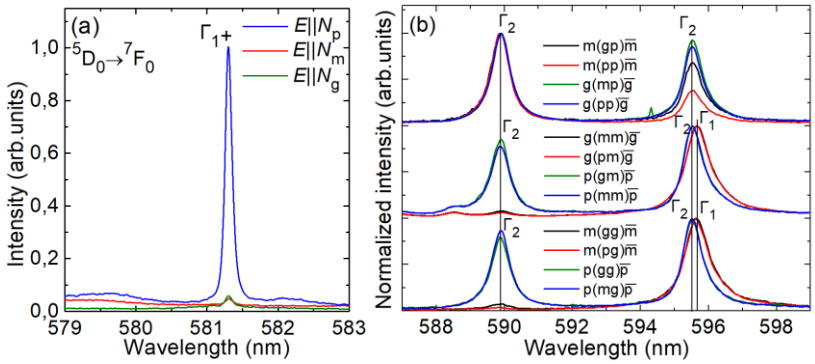

Figure 4. Polarization anisotropy of emission corresponding to the $^5D_0 \rightarrow {}^7F_{0,1}$ transitions of Eu^{3+} ions in $KY(WO_4)_2$: **(a)** ED and MD forbidden $^5D_0 \rightarrow {}^7F_0$ transition; **(b)** MD allowed transition $^5D_0 \rightarrow {}^7F_1$, Porto's notations are used. "+" marks electronic transitions, $\Gamma_{1(2)}$ – irreducible representations corresponding to sub-levels of the ^7F_J multiplets.

Similar behavior was described and interpreted previously for MD transitions in emission of rare-earth ions in optically uniaxial (e.g., tetragonal) and optically biaxial (e.g., orthorhombic) crystals [14]. It has never been observed for monoclinic crystals. A MD transition is caused by an interaction of an active ion (Eu^{3+}, in our case) with the magnetic field component of the light through the magnetic dipole. The orientation of the latter is determined by the vector $\boldsymbol{M}$. Thus, the orientation of the magnetic field vector $\boldsymbol{H}$ of radiation with respect to $\boldsymbol{M}$ becomes relevant.

According to Table 1, the $^5D_0$ multiplet consists of a single sub-level (Γ_1). The $^7F_1$ multiplet contains three sub-levels, denoted as Γ_1 and $\Gamma_2^{(1)}$, $\Gamma_2^{(2)}$. The probability of a MD transition in emission is proportional to $|\boldsymbol{e}_{\rho k} \cdot [\boldsymbol{k} \times \langle f|\boldsymbol{M}|i\rangle]|^2$, where $\boldsymbol{e}_{\rho k}$ is the polarization vector, $\boldsymbol{k}$ is the Poynting vector and *f* and *i* indices mark the initial (*i*) and final (*f*) Stark sub-levels [14]. The vector product in square brackets is maximized when $\boldsymbol{k} \perp \boldsymbol{M}$ and the whole mixed product is maximized when all three vectors are mutually orthogonal. From these considerations, polarization selection rules for the MD $^5D_0 \rightarrow {}^7F_1$ transition are obtained, see Table 3.

Table 3. Polarization selection rules for the pure MD $^5D_0 \rightarrow {}^7F$ transition of Eu^{3+} ions in C_2 sites in the monoclinic $KY(WO_4)_2$ crystal.

$\boldsymbol{M}$ vector	$^5D_0 \rightarrow {}^7F_1$	Preferred $\boldsymbol{k}$	Possible $\boldsymbol{e}_{\rho k}$
$\boldsymbol{M} \parallel C_2$ ($\boldsymbol{M} \parallel p$)	$\Gamma_1 \rightarrow \Gamma_1$	$\parallel g$	$\parallel m$
		$\parallel m$	$\parallel g$
$\boldsymbol{M} \perp C_2$ ($\boldsymbol{M} \parallel g, m$)	$\Gamma_1 \rightarrow \Gamma_2^{(1)},\Gamma_2^{(2)}$	$\parallel p$	$\parallel g, m$
		$\parallel g$	$\parallel p, m$
		$\parallel m$	$\parallel p, g$

Let us analyze Figure 4(b) using Table 3. All the four spectra from the upper group (*m*(*gp*)*m*, etc.) correspond to the $\Gamma_1 \rightarrow \Gamma_2^{(1)},\Gamma_2^{(2)}$ selection rule (two emission lines are observed). For the intermediate group, two spectra (*g*(*mm*)*g* and *g*(*pm*)*g*) correspond to the selection rule $\Gamma_1 \rightarrow \Gamma_1$ (one line) the other two (*p*(*gm*)*p* and *p*(*mm*)*p*) – to the $\Gamma_1 \rightarrow \Gamma_2^{(1)},\Gamma_2^{(2)}$ one (two lines). Finally, for the lower group of spectra, two of them (*m*(*gg*)*m* and *m*(*pg*)*m*) correspond to the selection rule $\Gamma_1 \rightarrow \Gamma_1$ (one line) the other two (*p*(*gg*)*p* and *p*(*mg*)*p*) – to the $\Gamma_1 \rightarrow \Gamma_2^{(1)},\Gamma_2^{(2)}$ one (two lines). Thus, the measured spectra well agree with the constructed table of polarization selection rules for MD transitions.

The analysis of the $^5D_0 \rightarrow {}^7F_J$ transitions in emission of Eu^{3+} ions in $KY(WO_4)_2$ allowed us to construct the energy-level scheme. It is shown partially in Figure 5 focusing on the $^7F_{0\text{-}2}$ and $^5D_0$ states, as well as the corresponding emission wavelengths.

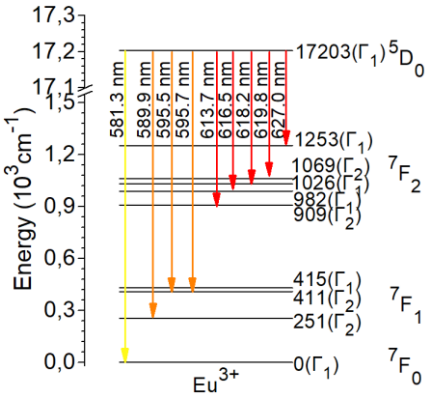

Figure 5. Crystal-field splitting of $^5D_0$ and $^7F_{0\text{-}2}$ Eu^{3+} multiplets for the monoclinic Eu:$KY(WO_4)_2$ crystal, *arrows* indicate the transitions in emission.

4. Conclusion

Eu^{3+} ions embedded in low-symmetry sites (C_2) in monoclinic crystals such as $KY(WO_4)_2$ exhibit strong polarization anisotropy of their emission properties. The nature of the $^5D_0 \rightarrow {}^7F_J$ electronic transitions (ED or MD) has a direct consequence on the polarization selection rules. The anisotropy of the emission due to the pure ED transitions terminating at the $^7F_2$ and $^7F_4$ states is determined by the orientation of the ***E*** vector with respect to the 2-fold symmetry axis of the crystal. These transitions are of interest for laser emission in the red and deep-red ranges. The anisotropic emission properties corresponding to the pure MD transition terminating at the $^7F_1$ state are determined by the orientation of the ***H*** vector. The description of this transition is important for the "structural probe" analysis.

Acknowledgments

The reported study was funded by RFBR, project number 19-32-90199. It was also supported by Spanish Government, Ministry of Science and Innovation (project No. PID2019-108543RB-I00) and by Generalitat de Catalunya (project No. 2017SGR755).

References

[1] Huang X, Guo H, Li B 2017 *J. Alloys Compd.* **720** 29
[2] Zhu H, Fang M, Huang Z, Liu Y G, Chen K, Min X, Mao Y, Wang M 2016 *J. Lumin.* **172** 180
[3] Kim K B, Kim Y I, Chun H G, Cho T Y, Jung J S, Kang J G 2002 *Chem. Mater.* **14** 5045
[4] Binnemans K, and Görller-Walrand C 1996 *J. Rare Earths* **14** 173
[5] Loiko P A, Rachkovskaya G E, Zakharevich G B, Kornienko A A, Dunina E B, Yasukevich A S, Yumashev K V 2014 *J. Non-Cryst. Solids* **392** 39
[6] Dashkevich V, Bagayev S, Orlovich V, Bui A, Loiko P, Yumashev K, Yasukevich A, Kuleshov N, Vatnik S, Pavlyuk A 2015 *Laser Phys. Lett*. **12** 085001
[7] Demesh M, Yasukevich A, Kisel V, Dunina E, Kornienko A, Dashkevich V, Orlovich V, Castellano-Hernández E, Kränkel C, Kuleshov N 2018 *Opt. Lett.* **43** 2364
[8] Bagayev S, Dashkevich V, Orlovich V, Vatnik S, Pavlyuk A, Yurkin A 2011 *Quantum Electron*. **41** 189
[9] Loiko P, Rytz D, Schwung S, Pues P, Jüstel T, Doualan J-L, Camy P 2021 *Opt. Lett*. **46** 2702
[10] Loiko P, Dashkevich V, Bagaev S, Orlovich V, Yasukevich A, Yumashev K, Kuleshov N, Dunina E, Kornienko A, Vatnik S, Pavlyuk A 2014 *J. Lumin* **153** 221
[11] Loiko P A, Yumashev K V, Kuleshov N V, Pavlyuk A A 2012 *Appl. Phys. B* **106** 663
[12] Shannon R D 1976 *Acta Cryst. A* **32** 751
[13] Aull B F, Jenssen H P 1982 *IEEE J. Quantum Electron*. **18** 925
[14] Volokitina A, Loiko P, Vilejshikova E, Mateos X, Dunina E, Kornienko A, Kuleshov N, Pavlyuk A 2018 *J. Alloys Compd*. **762** 786